General Relativity and Gravitation (2025) 57:41
https://doi.org/10.1007/s10714-025-03359-4

RESEARCH

Non-static axisymmetric structures embedded in an asymptotically ΛCDM universe

Gonzalo García-Reyes[1]

Received: 17 September 2024 / Accepted: 9 January 2025

Abstract

We construct non-static adiabatic axisymmetric structures embedded in an asymptotically ΛCDM universe from given solutions of the Poisson's equation of Newtonian gravity, using a particular form of the metric in isotropic coordinates. The approach is used in building of a razor-thin disk source made of perfect fluid for the McVittie metric, a system composite by a Plummer-type perfect fluid razor-thin disk surrounded by an halo also of perfect fluid, and a model of Miyamoto–Nagai-type anisotropic fluid thick disks, embedded in an asymptotic ΛCDM universe. In the especial case of spherical symmetry, we also present a family of models of expanding anisotropic thick spherical shells. Moreover, the geodesic motion of test particles in stable circular orbits around of the structures, the fulfilment of the energy conditions and principal stresses (pressure) are analyzed.

Keywords General relativity · Non-static axisymmetric spacetimes · ΛCDM cosmology

Contents

✉ Gonzalo García-Reyes
ggarcia@utp.edu.co

[1] Departamento de Física, Universidad Tecnológica de Pereira, A. A. 97, Pereira, Colombia

Published online: 12 February 2025

1 Introduction

Axially symmetric matter configurations play an important role in astrophysics as models of certain galaxies and stars, accretion disks, and in general relativity as sources of vacuum gravitational fields and in the description of accretion disks around black holes which are genuinely relativistic objects. In particular disk-shaped matter distributions can also be useful in modeling of flattened cosmic structures given the evidence of thin and flat sheet-like patterns present in the large-scale structure of the Universe, which constitute an interesting challenge for the lambda-cold dark matter cosmology [1]. Such flattened systems are well known as the Local Supercluster [2] and the Local Sheet [3]. On the other hand, in astrophysics expanding spherical shell-like system model supernovae and in cosmology one of the possible motivations for the study of shells is the observations of spherical shell-like structures (bubbles) in the distribution of galaxies in our cosmic neighbourhood, which are interpreted as a signatures of the baryon acoustic oscillations generated in the hot plasma of the early universe [4, 5]. Although within the framework of general relativity the expansion of the universe can be universal on all scales [6–11], it is also known that the magnitude of its effect is essentially negligible for local systems and its detection is beyond current technological capabilities [12]. However, the overall cosmic expansion can affect the dynamics of local gravitational systems, such as the rotation and stability of the galaxies, as indicated by simulations of galaxies [13].

In general relativity, axially symmetric solutions of Einstein's field equations representing the field of an infinitesimally thin disk have been extensively studied. These solutions can be static or stationary and with or without radial pressure. Solutions corresponding to static thin disks without radial pressure were first studied by Bonnor and Sackfield [14], and Morgan and Morgan [15], and with radial pressure also by Morgan and Morgan [16]. Several classes of exact solutions of the Einstein field equations corresponding to static thin disks with or without radial pressure have been obtained by different authors [17–23]. Rotating thin disks that can be considered as a source of a Kerr metric were presented by Bičák and Ledvinka [24], while rotating disks with heat flow were studied by González and Letelier [25]. The exact superposition of a disk and a static black hole was first considered by Lemos and Letelier [26, 27]. Models of static perfect fluid disks with halos were investigated in [28]. Non-static axisymmetric exact solutions of the Einstein's equations describing thin disks embedded in an expanding Friedmann–Lemaître–Robertson–Walker (FLRW) universe were discussed in [29]. These disks have no radial pressure and in order to build stable models are interpretated as two counterrotating dust fluids. Relativistic thick disk models have also been constructed in the static case in references [30–32] and rotating thick disks in [33]. Meanwhile, relativistic models of thick spherical shells were studied in [34–36].

The purpose of this paper is to build non-static adiabatic axisymmetric structures embedded in an asymptotically ΛCDM universe from several seed Newtonian potential-density pairs, using a particular form of the metric in isotropic coordinates. These spacetimes contain two unknown metric functions. One of the metric functions is obtained of the fact that one of the field equations is a Poisson type non-static and non-linear equation. This equation is solved by demanding that in Newtonian approxi-

mation the relativistic energy density reduces to its Newtonian value. The other metric function, which describes the temporal dependence of spacetime, is obtained in this work assuming a specific asymptotic cosmological model, the standard ΛCDM cosmology.

The paper is organized as follows. In Sect. 2 we summarize the method to build different adiabatic axially symmetric matter configurations embedded in an asymptotically ΛCDM universe from given solutions of Poisson's equation. We also analysis the geodesic circular motion of test particles moving around the structures on the equatorial plane and the stability of the orbits against radial perturbations. In Sect. 3, we review the "displace, cut and reflect" method used to construct thin disks and disks with halos from known solutions of Einstein field equations and its generalizations to model thick disks. In Sects. 4–7, the approach is used in building of a perfect fluid disk like source for the McVittie's inhomogeneous cosmological solution, a system composite by a Plummer-type perfect fluid thin disk surrounded by a perfect fluid halo, a model of Miyamoto–Nagai-type anisotropic fluid thick disks, and in the especial case of spherical symmetry, we also present a family of models of anisotropic thick spherical shells, embedded in an asymptotic ΛCDM universe, respectively. Finally, Sec. 8 is devoted to discussion of the results.

2 Poisson type non-static axisymmetric structures

The line element for a spherically symmetric spacetime in isotropic coordinates is given by [37, 38]

$$ds^2 = e^{2\nu}c^2dt^2 - e^{2\lambda}(dr^2 + r^2d\Omega^2), \tag{1}$$

where $d\Omega^2 = d\theta^2 + \sin^2\theta d\varphi^2$ is the metric on a unit 2-sphere, and ν, λ are functions of t and r. In cylindrical coordinates (t, φ, R, z) the same metric reads

$$ds^2 = -e^{2\nu}dt^2 + e^{2\lambda}(R^2d\varphi^2 + dR^2 + dz^2), \tag{2}$$

where ν, λ are now functions of t, R and z. Now let's consider the above metric in the particular form [39]

$$ds^2 = -\left(\frac{1-f}{1+f}\right)^2 dt^2 + (1+f)^4\, S(t)^2(R^2d\varphi^2 + dR^2 + dz^2), \tag{3}$$

where $f(R, z, t)$. Einstein's gravitational field equations (with $c = 1$) $G_{ab} = 8\pi G T_{ab}$ yield the following non-zero components of the energy-momentum tensor

$$8\pi G T^t_t = -3H^2 + \frac{4(f_{,RR} + R^{-1}f_{,R} + f_{,zz})}{S(t)^2(1+f)^5}, \tag{4a}$$

$$8\pi G T^\varphi_\varphi = -3H^2 - 2\dot{H}\left(\frac{1+f}{1-f}\right) + \frac{2\left[(f_{,R})^2 + (f_{,z})^2 - f(f_{,RR} + f_{,zz})\right]}{S(t)^2(1+f)^5(1-f)}, \tag{4b}$$

$$8\pi G T^{R}_{R} = -3H^2 - 2\dot{H}\left(\frac{1+f}{1-f}\right) + \frac{2\left[(f_{,z})^2 - 2(f_{,R})^2 - f f_{,zz} - R^{-1} f f_{,R}\right]}{S(t)^2(1+f)^5(1-f)}, \tag{4c}$$

$$8\pi G T^{z}_{z} = -3H^2 - 2\dot{H}\left(\frac{1+f}{1-f}\right) + \frac{2\left[(f_{,R})^2 - 2(f_{,z})^2 - f f_{,RR} - R^{-1} f f_{,R}\right]}{S(t)^2(1+f)^5(1-f)}, \tag{4d}$$

$$8\pi G T^{R}_{z} = \frac{2\left[f f_{,Rz} - 3 f_{,R} f_{,z}\right]}{S(t)^2(1+f)^5(1-f)}, \tag{4e}$$

where $(\,)_{,R} \equiv \partial/\partial R$, $(\,)_{,RR} \equiv \partial^2/\partial R^2$, etc., and

$$H = \frac{\dot{S}(t)}{S(t)}, \tag{5}$$

where a dot denotes differentiation with respect to t. In a cosmological setting ($f = 0$) this function represents the Hubble parameter, and $S(t)$ the scale factor.

Now, in order to analyze the matter distributions is necessary to compute the eigenvalues and eigenvectors of the energy-momentum tensor. The eigenvalue problem for the energy-momentum tensor (4a)–(4e) has the solutions

$$\lambda_t = T^{t}{}_{t}, \tag{6a}$$

$$\lambda_\varphi = T^{\varphi}{}_{\varphi}, \tag{6b}$$

$$\lambda_\pm = \frac{T \pm \sqrt{D}}{2}, \tag{6c}$$

where $\lambda_+ = \lambda_R$, $\lambda_- = \lambda_z$ and

$$T = T^{R}{}_{R} + T^{z}{}_{z}, \tag{7a}$$

$$D = (T^{R}{}_{R} - T^{z}{}_{z})^2 + 4(T^{R}{}_{z})^2. \tag{7b}$$

The corresponding eigenvectors define the orthonormal tetrad $\mathrm{e}_{(a)}{}^{b} = \{V^b, X^b, Y^b, Z^b\}$, where

$$V^a = \frac{1}{\sqrt{-g_{tt}}}(1,0,0,0), \tag{8a}$$

$$X^a = \frac{1}{\sqrt{g_{\varphi\varphi}}}(0,1,0,0), \tag{8b}$$

$$Y^a = \frac{1}{\sqrt{g_{RR}\left(1+n_+^2\right)}}(0,0,1,n_+), \tag{8c}$$

$$Z^a = \frac{1}{\sqrt{g_{RR}\left(1+n_-^2\right)}}(0,0,1,n_-), \tag{8d}$$

where

$$n_{\pm} = \frac{T^{z}{}_{z} - T^{R}{}_{R} \pm \sqrt{D}}{2T^{R}{}_{z}}. \tag{9}$$

In terms of the above proper observer, the energy density is given by $\rho = -\lambda_t$ and the principal stresses by $p_i = \lambda_i$ $(i = \varphi, R, z)$. When the energy-momentum tensor is diagonal $p_i = T^i_{\ i}$ and the orthonormal basis takes the simple form

$$V^a = e^{-\psi}\delta^a_t, \quad X^a = e^{-\lambda}\delta^a_\varphi/R, \tag{10a}$$

$$Y^a = e^{-\lambda}\delta^a_R, \quad Z^a = e^{-\lambda}\delta^a_z. \tag{10b}$$

Now, by taking $f = -\frac{\phi(R,z)}{2S(t)}$ we get, even without spatial symmetry, for the energy density the following Poisson type non-static and non-linear equation

$$8\pi G\rho = 3H^2 + \frac{2\nabla^2\phi}{S(t)^3\left(1 - \frac{\Phi}{2S(t)}\right)^5}. \tag{11}$$

In fact, in Newtonian approximation $\phi \ll 1$ and setting $S(t_0) = 1$ today it reduces to Poisson's equation, $\nabla^2\Phi = 4\pi G\rho_N$. This equation can be solved by guessing the metric function ϕ. A physically reasonable way to choose the potential ϕ is by requiring that in the Newtonian approximation the energy density reduces to its Newtonian value ρ_N. This condition is satisfied by taking $\phi = \Phi$. Therefore,

$$8\pi G\rho = 3H^2 + \frac{8\pi G\rho_N}{S(t)^3\left(1 - \frac{\Phi}{2S(t)}\right)^5}. \tag{12}$$

So this approach allows building different non-static adiabatic axisymmetric structures from seed Newtonian potential-density pairs (Φ, ρ_N). The other metric function $S(t)$ can be obtained, adopted here, for example by assuming an asymptotic cosmological model. In that case, these spacetimes may be interpreted as Poisson type local inhomogeneities, that is, in weak-field limit $\phi \ll 1$ and $S(t_0) = 1$ such structures are gravitationally described by Newton's theory, embedded in a flat FLRW universe. Other possibility, explored in reference [39], is via constructing of a gravitational collapse model.

2.1 ΛCDM model

The metric function $S(t)$ will be chosen is such a way that we obtain non-static axisymmetric structures that asymptote to the standard ΛCDM cosmology which is in accordance with current observations showing an accelerated expansion of the Universe [40]. Thus, for a spatially flat universe with nonrelativistic matter (cold

dark and baryonic matter) and dark energy in the form of a cosmological constant (neglecting the radiation content of the universe), the Friedmann equation reads

$$\frac{H^2}{H_0^2} = \Omega_m S^{-3} + \Omega_\Lambda, \tag{13}$$

where Ω_m is the present density parameter of pressureless matter, $\Omega_\Lambda = 1 - \Omega_m$ is the present dark energy density parameter and H_0 is the Hubble's constant. Assuming the base-ΛCDM cosmology, the latest measurement [40] gives $H_0 = (67.4 \pm 0.5)$ Km s^{-1} Mpc^{-1} and $\Omega_m = 0.315 \pm 0.007$. It is follows that

$$\frac{\dot{H}}{H_0^2} = -\frac{3}{2}\Omega_m S^{-3}. \tag{14}$$

For flat universe with a positive cosmological constant ($\Omega_m < 1$), the Friedmann equation (13) has the analytic solution [41]

$$S(t) = (\Omega_m/\Omega_\Lambda)^{1/3}\left(\sinh\left[\frac{3}{2}\sqrt{\Omega_\Lambda}H_0 t\right]\right)^{2/3}. \tag{15}$$

Such a spacetime asymptotically approaches the matter-dominated (Einstein-de Sitter universe) and dark-energy-dominated (de Sitter universe) eras at early and late times, respectively. Approximating the density parameter for the current matter as $\Omega_m = 0.31$, the age at which matter and the cosmological constant had equal energy density, measured in units of the Hubble time ($t_{\rm H} \equiv H_0^{-1}$) $\tilde{t} = H_0 t$, is $\tilde{t}_{m\Lambda} = 0.707$ and the age of the universe is $\tilde{t}_0 = 0.955$ [42]. For the Hubble parameter we obtain

$$H = \sqrt{\Omega_\Lambda}H_0 \coth\left[\frac{3}{2}\sqrt{\Omega_\Lambda}H_0 t\right]. \tag{16}$$

For spacetimes that asymptote to the standard ΛCDM cosmology we have

$$\bar{T}^t_t = -\Omega_\Lambda \coth^2\left[\frac{3}{2}\sqrt{\Omega_\Lambda}H_0 t\right] + \frac{4(f_{,RR} + R^{-1}f_{,R} + f_{,zz})}{3H_0^2 S(t)^2(1+f)^5}, \tag{17a}$$

$$\bar{T}^\varphi_\varphi = -\Omega_\Lambda + \left(\frac{2}{f^{-1}-1}\right)\Omega_m S(t)^{-3} + \frac{2\left[(f_{,R})^2 + (f_{,z})^2 - f(f_{,RR} + f_{,zz})\right]}{3H_0^2 S(t)^2(1+f)^5(1-f)}, \tag{17b}$$

$$\bar{T}^R_R = -\Omega_\Lambda + \left(\frac{2}{f^{-1}-1}\right)\Omega_m S(t)^{-3} + \frac{2\left[(f_{,z})^2 - 2(f_{,R})^2 - ff_{,zz} - R^{-1}ff_{,R}\right)}{3H_0^2 S(t)^2(1+f)^5(1-f)}, \tag{17c}$$

$$\tilde{T}^z_z = -\Omega_\Lambda + \left(\frac{2}{f^{-1}-1}\right)\Omega_m S(t)^{-3} + \frac{2\left[(f_{,R})^2 - 2(f_{,z})^2 - ff_{,RR} - R^{-1}ff_{,R}\right]}{3H_0^2 S(t)^2(1+f)^5(1-f)}, \tag{17d}$$

$$\bar{T}^{R}_{\ z} = \frac{2\left[ff_{,Rz} - 3f_{,R}f_{,z}\right]}{3H_0^2 S(t)^2(1+f)^5(1-f)}, \tag{17e}$$

where the dimensionless quantities are $\bar{T}^{a}_{\ b} = T^{a}_{\ b}/\rho_{cr}$, where $\rho_{cr} = \frac{3H_0^2}{8\pi G}$ is the critical energy density. The first terms on the right-hand side of equations (17a)–(17d) describe the ΛCDM universe, the last terms of the energy-momentum tensor are the components of an expanding matter configuration (local inhomogeneities) in such universe, and the second terms in equations (17b)–(17d) represent the interaction between the matter of the cosmological medium and the expanding matter distributions. Such energy-momentum tensor can be written as $T_{ab} = T^{\Lambda\text{CDM}}_{ab} + T^{\text{int}}_{ab} + T^{\text{inh}}_{ab}$ and the spacetime can be interpreted as an expanding matter distribution in a ΛCDM universe.

In order to have physically reasonable expanding matter configurations we will assume that the energy-momentum tensor T^{inh}_{ab} satisfies the energy conditions [43]. The weak energy condition states that $\rho \geq 0$, whereas the strong energy condition, which ensures that gravity will always be attractive, reads $\rho_{eff} = \rho + p_\varphi + p_R + p_z \geq 0$, where ρ_{eff} is the "effective Newtonian density". The dominant energy condition requires that $\rho \geq |p_i|$. The latter condition is equivalent to requiring that the local speed of sound is not greater than local speed of light. Furthermore, since we are mainly interested in modeling inhomogeneities as a fluid made of ordinary baryonic matter that makes up stars, galaxies, clusters of galaxies, for instance, and which presents positive stresses (pressure), we will also assume positive values for the principal stresses. The same consideration is made for the interaction term.

2.2 Stable circular equatorial orbits

A important parameter related to the motion of test particles around the structures on the equatorial plane is circular speed (rotation curves) v_c. For instance, the stars of the disk in spiral galaxies travel in nearly circular orbits around the galactic center [44]. So for circular, equatorial orbits the 4-velocity $\mathbf{u}$ of the particles with respect to the coordinates frame has components $\mathbf{u} = u^t(1, \omega, 0, 0)$, where $\omega = u^\varphi/u^t = \frac{d\varphi}{dt}$ is the angular speed of the test particles. In turn, with respect to the tetrad frame (8a)–(8d) the 4-velocity has components

$$u^{(a)} = e^{(a)}_{\ \ b} u^b, \tag{18}$$

while the 3-velocity

$$v^{(i)} = \frac{u^{(i)}}{u^{(t)}} = \frac{e^{(i)}_{\ \ a} u^a}{e^{(t)}_{\ \ b} u^b}. \tag{19}$$

In the especial case of circular orbits on the equatorial plane the only non-vanishing 3-velocity component is $v^{(\varphi)}$, and is given by

$$[v^{(\varphi)}]^2 = v_c^2 = -\frac{g_{\varphi\varphi}}{g_{tt}}\omega^2, \tag{20}$$

where v_c represents the circular speed profile of the particle as seen by an observer at infinity. The angular speed ω can be calculated considering the geodesic motion of the particles. For circular orbits on the plane equatorial of the structures the Lagrangian for a massive test particle moving in the background metric (2) is

$$2\mathcal{L} = g_{ab}u^a u^b = -e^{2\nu}(u^t)^2 + e^{2\lambda}R^2(u^\varphi)^2, \tag{21}$$

and the Lagrange's equations

$$\frac{d}{d\tau}\left(\frac{\partial\mathcal{L}}{\partial u^a}\right) - \frac{\partial\mathcal{L}}{\partial x^a} = 0 \tag{22}$$

yield the radial motion's equation

$$g_{tt,R}(u^t)^2 + g_{\varphi\varphi,R}(u^\varphi)^2 = 0. \tag{23}$$

Then we obtain

$$\omega^2 = -\frac{g_{tt,R}}{g_{\varphi\varphi,R}}, \tag{24}$$

and the circular speed is given by

$$v_c^2 = \frac{R\nu_{,R}}{1 + R\lambda_{,R}}. \tag{25}$$

For the metric (3) has

$$v_c^2 = \frac{v_N^2/S(t)}{(1-f)\left(1 + f - v_N^2/S(t)\right)}, \tag{26}$$

where $v_N^2 = R\Phi_{,R}$ is the Newtonian circular speed.

To analyze the stability of the particles against radial perturbations we can use an extension of the Rayleigh criteria of stability of a fluid in rest in a gravitational field [45–47]

$$\frac{d(h^2)}{dR} > 0, \tag{27}$$

where h is the specific angular momentum, defined as $h = p_\varphi/m = g_{\varphi\varphi}u^\varphi = g_{\varphi\varphi}\omega u^t$, where $p_\varphi = \partial\mathcal{L}/\partial u^\varphi$ and u^t obtains normalizing u^a, that is requiring $g_{ab}u^a u^b = -1$, so that

$$(u^t)^2 = -\frac{1}{g_{\varphi\varphi}\omega^2 + g_{tt}}. \tag{28}$$

Thus, for circular, planar orbits we obtain

$$h^2 = \frac{R^2(1+f)^4 v_c^2}{1-v_c^2}. \tag{29}$$

3 Relativistic expanding disk like axisymmetric structures

Solutions of the Einstein's field equations representing the gravitational field of a disk of infinitesimal thickness can be constructed assuming the components of the metric tensor continuous across the disk and its first derivatives discontinuous in the direction normal to the disk. Such discontinuity in the metric can be introduced by a Kuzmin–Toomre transformation $z \to a + |z|$, where a is a positive constant, which was first used by Kuzmin [48] and Toomre [49] to constructed Newtonian models of thin disks, and later extended to general relativity [21, 22, 24, 25]. This method also is known in literature as "displace, cut and reflect" method, where a is the cut parameter. The method is the gravitational version of the method of images of electrostatic. The disk models built using this method are of infinite extension, however, since the energy density decreases rapidly it is always possible, in principle, to define a cut-off radius and consider the disks as finite. This procedure in principle can be applied to any solution of the Einstein equations with or without energy-momentum tensor. In particular, when this procedure is applied to a spherical matter distribution of radius $r_{sph} > a$ the result is a system composite by a thin disk surrounded by a halo of matter [28]. On the other hand, models of thick disks in general relativity can be obtained by a Miyamoto–Nagai transformation used in Newtonian gravity to generate three-dimensional potential-density pairs from the Kuzmin–Toomre thin disks [50, 51]. This procedure is equivalent to change in the Kuzmin–Toomre disks $|z| \to \sqrt{z^2 + b^2}$, where b is a positive parameter. The models describe the stratification of mass in the central bulge as well in the disk part of galaxies.

In the case of thin disks, its content of matter can be analyzed by using the formalism of distributions in curved spacetimes [52–54] or the junction conditions on the extrinsic curvature of thin shells [55, 56]. The Einstein equations give us

$$G_{ab} = 8\pi G(T_{ab} + T_{ab}^{\text{disk}}) = 8\pi G(T_{ab} + Q_{ab}\,\delta(z)) \tag{30}$$

where $\delta(z)$ is the Dirac delta function with support on the disk, T_{ab} is the energy-momentum tensor above and below the plane of the disk, and

$$Q_b^a = \frac{1}{16\pi}\{b^{az}\delta_b^z - b^{zz}\delta_b^a + g^{az}b_b^z - g^{zz}b_b^a + b_c^c(g^{zz}\delta_b^a - g^{az}\delta_b^z)\} \tag{31}$$

is the distributional energy-momentum tensor of the disk, where b_{ab} denote the discontinuities (or jump) in the first derivatives of the metric tensor on the plane $z = 0$,

$$b_{ab} = [g_{ab,z}] = g^+_{ab,z}|_{z=0} - g^-_{ab,z}|_{z=0} = 2\, g^+_{ab,z}|_{z=0}. \tag{32}$$

The "true" surface energy-momentum tensor (SEMT) of the disk, τ_{ab}, can be obtained through the relation

$$\tau_{ab} = \int Q_{ab}\delta(z)\, ds_n = \sqrt{g_{zz}}Q_{ab}, \tag{33}$$

where $ds_n = \sqrt{g_{zz}}\, dz$ is the "physical measure" of length in the direction normal to the disk. In particular, for the metric (3), with $f = -\frac{\phi(R,z)}{2S(t)}$, the nonzero components of τ_a^b are

$$\tau_t^t = -\frac{\sigma_N}{S(t)^2\,(1+f)^3} \tag{34a}$$

$$\tau_\varphi^\varphi = \tau_R^R = -\frac{ff_{,z}}{2\pi G S(t)(1-f)(1+f)^3}, \tag{34b}$$

where $\sigma_N = \Phi_{,z}/(2\pi G)$ is the Newtonian surface density, and, in terms of the comoving observer (10a)–(10b), the SEMT takes the form of a perfect fluid

$$\tau^{ab} = (p+\sigma)V^a V^b + pg^{ab}, \tag{35}$$

where

$$\sigma = -\tau_t^t, \quad p = p_\varphi = p_R = \tau_\varphi^\varphi, \tag{36}$$

are, respectively, the surface energy density σ and the azimuthal and radial stresses p on the disk. All above quantities are evaluated at $z = 0^+$. In this case the energy conditions read $\sigma \geq 0$, $\sigma + 2p \geq 0$, and $|\sigma| \geq |p|$. So for a given flattened potential-density pair (Φ, σ_N), the energy-momentum tensor of spacetimes that asymptote to the standard ΛCDM cosmology can be written as $T_{ab} = T_{ab}^{\Lambda\text{CDM}} + T_{ab}^{\text{int}} + T_{ab}^{\text{halo}} + T_{ab}^{\text{disk}}$ and the solution can be interpreted as a expanding halo + perfect fluid disk system in a ΛCDM universe.

4 Kuzmin-type perfect fluid thin disks embedded in a ΛCDM universe

A simple perfect fluid solution of Einstein's field equations for the line element (3) is the McVittie metric [57] which obtains in isotropic spherical coordinates from Newtonian spherical potential of a point mass

$$\Phi = -\frac{GM}{r}, \tag{37}$$

where $r = \sqrt{R^2+z^2}$, M is the mass of the source and $S(t)$ is the asymptotic cosmological scale factor. For $S = 1$ the line element reduces to the Schwarzschild spacetime in isotropic coordinates and for $M = 0$ to the flat FLRW universe. This

metric describes a central spherical object embedded in an expanding FLRW cosmological spacetime [58–60]. When $S(t) = e^{\sqrt{\frac{\Lambda}{3}}t}$ the McVittie metric is the Kottler spacetime in isotropic coordinates which for $\Lambda > 0$ it is also called the Schwarzschild-de Sitter metric and for $\Lambda < 0$ the Schwarzschild-anti-de Sitter metric. Moreover, in the limit $GM/(2Sr) \ll 1$ the McVittie metric reduces to a perturbed FLRW universe with zero curvature.

Energy density and isotropic pressure are given by

$$8\pi G\rho = 3H^2, \tag{38a}$$

$$8\pi GP = -3H^2 - 2\dot{H}\left(\frac{1+f}{1-f}\right), \tag{38b}$$

where

$$f = \frac{GM}{2S(t)r}. \tag{39}$$

Moreover, the McVittie solution has a curvature singularity at $r = r_S/S(t)$, where $r_S = GM/2$, as can be seen from the Ricci scalar which is given by $R = 12\,H^2 + 6\dot{H}\left(\frac{1+f}{1-f}\right)$, where the pressure also goes to infinity.

For the McVittie solution has

$$\bar{\rho} = \Omega_\Lambda \coth^2\left[\frac{3}{2}\sqrt{\Omega_\Lambda}H_0 t\right], \tag{40a}$$

$$\bar{P} = -\Omega_\Lambda + \left(\frac{2}{f^{-1}-1}\right)\Omega_m S(t)^{-3}, \tag{40b}$$

where the dimensionless quantities are $\bar{\rho} = \rho/\rho_{cr}$ and $\bar{P} = P/\rho_{cr}$, where $\rho_{cr} = \frac{3H_0^2}{8\pi G}$ is the critical energy density. The energy density together with the first term in the pressure represent the contribution of the ΛCDM universe whereas the inhomogeneous term in the pressure, $\bar{P}_{\rm int} = P_{\rm int}/\rho_{cr}$, describes the interaction between the matter presents in the cosmological medium and the mass source, and is a positive and non-singular quantity in the region $r > r_S/S(t)$. Indeed, when the mass M is absent or far away from the central object, the pressure due to matter is zero in agreement with the standard model of cosmology, so that the spacetime is homogeneous and the negative pressure is that caused only by the cosmological constant. It follows that the energy-momentum tensor can be written as $T_{ab} = T_{ab}^{\Lambda\rm CDM} + T_{ab}^{\rm int}$.

Now the application of the Kuzmin–Toomre transformation to the Kepler point-mass potential (37) yields the flattened potential-density pair

$$\Phi = -\frac{GM}{\sqrt{R^2 + (a+|z|)^2}}, \tag{41a}$$

$$\sigma_N = \frac{aM}{2\pi(R^2+a^2)^{3/2}}, \tag{41b}$$

where M is the mass of disk and a is a positive parameter representing the disk length scale. This pair corresponds to the Kuzmin's razor-thin disk system and is used in Newtonian gravity as an approximate model of spiral galaxies. The rotation curve is given by

$$v_{cN}^2 = \frac{GMR^2}{(R^2+a^2)^{3/2}}. \tag{42}$$

For a spacetime that asymptotes to the standard ΛCDM cosmology, the energy-momentum tensor takes the form $T_{ab} = T_{ab}^{\Lambda\text{CDM}} + T_{ab}^{\text{int}} + T_{ab}^{\text{disk}}$, and the solution describes a Kuzmin-type perfect fluid thin disk embedded in an asymptotically ΛCDM universe and constitutes a disk-like source for the McVittie metric. The main physical quantities associated with the disks are

$$\tilde{\sigma} = \frac{\tilde{a}S(t)}{2\pi\left[S(t)\sqrt{\tilde{R}^2+\tilde{a}^2}+1\right]^3}, \tag{43a}$$

$$\tilde{p} = \frac{\tilde{a}S(t)}{4\pi\left[S(t)\sqrt{\tilde{R}^2+\tilde{a}^2}+1\right]^3\left(S(t)\sqrt{\tilde{R}^2+\tilde{a}^2}-1\right)}, \tag{43b}$$

$$v_c^2 = \frac{2\tilde{R}^2S(t)\sqrt{\tilde{R}^2+\tilde{a}^2}}{\left[S(t)(\tilde{R}^2+\tilde{a}^2)^{3/2}-\tilde{R}^2+\tilde{a}^2\right]\left(S(t)\sqrt{\tilde{R}^2+\tilde{a}^2}-1\right)}, \tag{43c}$$

$$\tilde{h}^2 = \frac{2\tilde{R}^4\left(S(t)\sqrt{\tilde{R}^2+\tilde{a}^2}+1\right)^4}{S(t)^3(\tilde{R}^2+\tilde{a}^2)^{3/2}\left[S(t)^2(\tilde{R}^2+\tilde{a}^2)^2-4S(t)\tilde{R}^2\sqrt{\tilde{R}^2+\tilde{a}^2}+\tilde{R}^2-\tilde{a}^2\right]} \tag{43d}$$

where the dimensionless quantities and parameters are $\tilde{R} = R/r_S$, $\tilde{a} = a/r_S$, $\tilde{\sigma} = (r_S^2/M)\sigma$, $\tilde{p} = (r_S^2/M)\,p$, and $\tilde{h} = h/r_S$. Equations (43a) and (43b) show that the weak energy condition is always satisfied, while the dominant and strong energy conditions hold in all the disk if $\tilde{a} \geq 3/(2\,S(t))$, with $S(t) \neq 0$ which is satisfactorily fulfilled for a big bang model for the evolution of the universe since the structures that we currently observe were formed after an initial state $t = 0$. This inequality also ensures that we have pressure everywhere on the disk and that the stresses associated with the interaction term P_{int} is also a positive and non-singular quantity. For disk like solutions that asymptotes to the de Sitter cosmology we have $\tilde{a} \geq (3/2)e^{\tilde{t}_0} = 3.898005874$. For a value of the parameter $\tilde{a}$, since $S(t)$ is a monotonically increasing function with time, this condition implies that physically realistic disk-like matter configurations are only possible from some minimum time $S(t^*) = 3/(2\tilde{a})$. However, such structures are still possible for $t < t^*$ by increasing the parameter $\tilde{a}$. It also means that physically acceptable Kuzmin-type perfect fluid disks in an expanding universe with a larger length scale today could be older.

In order to study the physical behavior of above quantities we perform a graphical analysis of them for the Kuzmin-type perfect fluid thin disk embedded in an asymptotically ΛCDM universe with parameter $\tilde{a} = 3$ at the dimensionless cosmic times

$\tilde{t} = \tilde{t}_{m\Lambda}, \tilde{t}_0$ (static case), and 1.2. In Fig. 1 we plot, as functions of $\tilde{R}$, the surface energy density $\tilde{\sigma}$, the isotropic pressure $\tilde{p}$, the circular speed (rotation curves) v_c^2 and the specific angular momentum $\tilde{h}^2$. We see that physical quantities decrease everywhere on the disk during expansion, but exhibits at all times a behavior similar to the static case. The same behavior is observed for other values of parameter $\tilde{a}$. So these disks becomes less dense as time passes and, just like static case, the energy density decreases rapidly enough to, in principle, define a cut off radius and consider the disk as finite when it expands. We observer that all the energy conditions are satisfied with $\tilde{t}^* = 0.4058181549$. However, as mentioned above physically realistic disks can be obtained for $t < t^*$ increasing the parameter $\tilde{a}$. For example, for the disk with $\tilde{a} = 3.4$ obtains that $\tilde{t}^* \approx 0.34$ which corresponds approximately to the epoch of formation of the Galactic thin disk [61].

We also find that for these parameter values the orbital speed of the particles around the disk is less than the speed of light in according to the dominant energy condition and we have stable orbits against radial perturbation, but like energy conditions one finds that these orbits are only possible from some minimum time. However, we still could have stable subluminal rotation curves for earlier times by increasing the length scale of the disk. The graphs also suggest that initially we have photonic orbits (radiation) and they become less relativistic and more stable as time goes on.

5 Plummer-type perfect fluid thin disks with haloes embedded in a ΛCDM universe

Another simple perfect fluid solution of Einstein's field equations for the line element (3) obtains from Plummer's spherical potential-density pair [62]

$$\Phi = -\frac{GM}{\sqrt{r^2 + b^2}}, \tag{44a}$$

$$\rho_N = \left(\frac{3M}{4\pi b^3}\right)\left(1 + \frac{r^2}{b^2}\right)^{-5/2}, \tag{44b}$$

where b is a non-zero constant with dimensions of length. Plummer's sphere is used in Newtonian gravity to model globular clusters, central spherical bulges of spiral galaxies and also as models of dark matter haloes. The orbital speed is

$$v_{cN}^2 = \frac{GMr^2}{\left(r^2 + b^2\right)^{3/2}}. \tag{45}$$

The relativistic version is an extension of the Buchdahl's static perfect fluid sphere [63], a relativistic analog of a classical polytrope of index 5, to the non-static case [39]. Energy density and isotropic pressure are given by

$$8\pi G\rho = 3H^2 + \frac{192b^2 S(t)^2}{(GM)^4\left[f^{-1} + 1\right]^5}, \tag{46a}$$

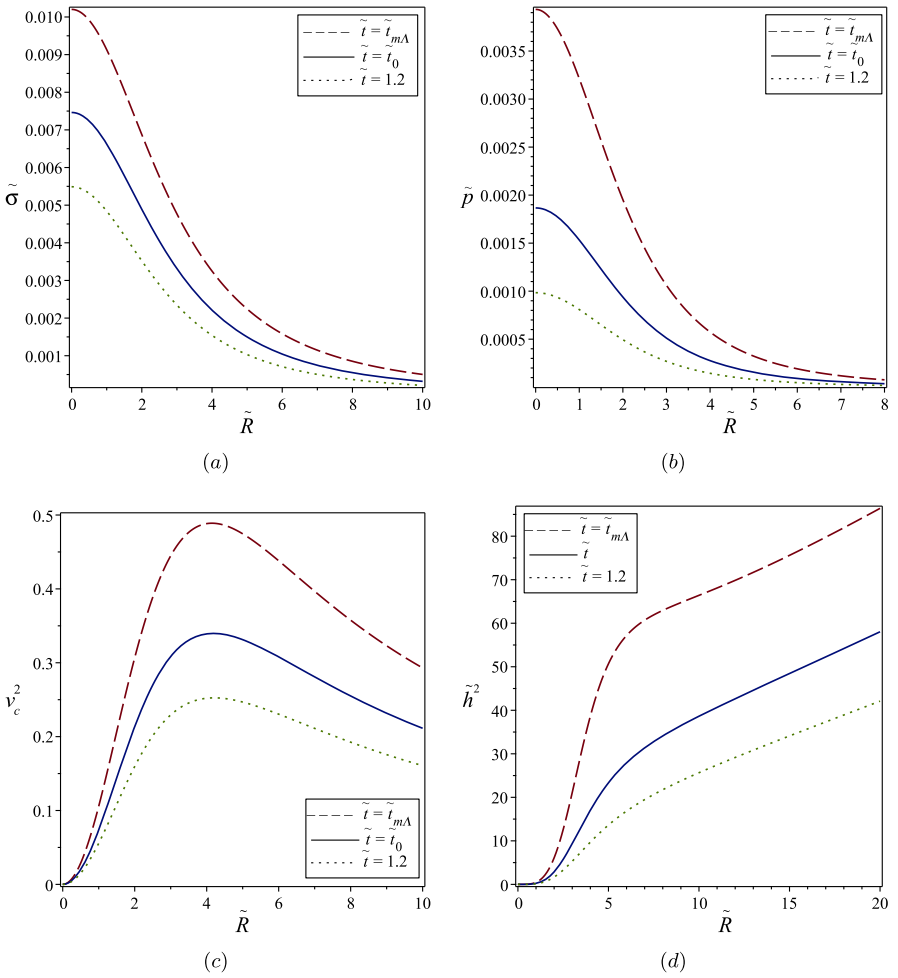

Fig. 1 **a** The surface energy density $\tilde{\sigma}$, **b** the pressure $\tilde{p}$, **c** the circular speed v_c^2 and **d** the specific angular momentum $\tilde{h}^2$ for the McVittie-type perfect fluid thin disk embedded in an asymptotically ΛCDM universe with parameter $\tilde{a} = 3$, and the dimensionless cosmic time $\tilde{t} = \tilde{t}_{m\Lambda}$ (dashed curves), $\tilde{t}_0$ (static case, solid curves), and 1.2 (dotted curves), as functions of $\tilde{R}$

$$8\pi GP = -3H^2 - 2\dot{H}\left(\frac{1+f}{1-f}\right) + \frac{64b^2S(t)^2}{(GM)^4(f^{-1}+1)^5(f^{-1}-1)}, \tag{46b}$$

with

$$f = \frac{GM}{2S(t)\sqrt{r^2+b^2}}. \tag{47}$$

For a solution that asymptotes to the standard ΛCDM cosmology we have

$$\bar{\rho} = \Omega_\Lambda \coth^2\left[\frac{3}{2}\sqrt{\Omega_\Lambda} H_0 t\right] + \frac{2GM\tilde{b}^2 S(t)^2}{H_0^2 r_S^3 \left(S(t)\xi + 1\right)^5}, \tag{48a}$$

$$\bar{P} = -\Omega_\Lambda + \left(\frac{2}{S(t)\xi - 1}\right)\Omega_m S(t)^{-3} + \frac{2GM\tilde{b}^2 S(t)^2}{3H_0^2 r_S^3 \left(S(t)\xi + 1\right)^5 \left(S(t)\xi - 1\right)}, \tag{48b}$$

where $\bar{\rho} = \rho/\rho_{cr}$, $\bar{P} = P/\rho_{cr}$, $\tilde{b} = b/r_S$ and $\xi = \sqrt{\tilde{r}^2 + \tilde{b}^2}$, with $\tilde{r} = r/r_S$. The first terms on the right-hand side of equations above represent the components of the ΛCDM universe, the last terms describe a relativistic expanding Plummer sphere in such universe and the second term in pressure represents the interaction between the matter of the cosmological medium and the relativistic Plummer sphere. So the energy-momentum tensor can be written as $T_{ab} = T_{ab}^{\Lambda\text{CDM}} + T_{ab}^{\text{int}} + T_{ab}^{\text{sph}}$ and the solution can be interpreted as an expanding Plummer sphere in a ΛCDM universe. We observer that the energy density always is a positive quantity in accordance with the weak energy condition while the strong and dominant energy conditions are satisfied in all the expanding sphere if holds the inequality $\tilde{b} \geq 4/(3\,S(t))$, with $S(t) \neq 0$. This condition also implies that the inhomogeneous terms in the stress are positive and non-singular quantities. In turn, the tangential speed and the specific angular momentum for circular orbits are given by

$$v_c^2 = \frac{2\tilde{r}^2 S(t)\xi}{\left(S(t)\xi^3 - \tilde{r}^2 + \tilde{b}^2\right)\left(S(t)\xi - 1\right)}, \tag{49a}$$

$$\tilde{h}^2 = \frac{2\tilde{r}^4 \left(S(t)\xi + 1\right)^4}{S(t)^3\xi^3\left(S(t)^2\xi^4 - 4\tilde{S}(t)\tilde{r}^2\xi + \tilde{r}^2 - \tilde{b}^2\right)}, \tag{49b}$$

where $\tilde{h} = h/r_S$. In Fig. 2 we have plotted, as function of $\tilde{r}$, the energy density $\tilde{\rho}_{\text{sph}} = (r_s^3/M)\rho_{\text{sph}}$, the pressure $\tilde{P}_{\text{sph}} = (r_s^3/M)P_{\text{sph}}$ for the relativistic expanding Plummer sphere and the quantities v_c^2 and $\tilde{h}$, with parameter $\tilde{b} = 3$ at the dimensionless cosmic times $\tilde{t} = \tilde{t}_{m\Lambda}, \tilde{t}_0$ (static case), and 1.2. These structures have no boundary, however, since energy density decreases rapidly is also possible, in principle, to define a cut-off radius (r_{sph}) and consider the matter distributions as finite. We also have stable circular orbits against radial perturbation.

Now when the Kuzmin transformation is applied to the Plummer potential (44a) the energy-momentum tensor takes the form $T_{ab} = T_{ab}^{\Lambda\text{CDM}} + T_{ab}^{\text{int}} + T_{ab}^{\text{halo}} + T_{ab}^{\text{disk}}$ and the solution can be interpreted as a system composite by a Plummer-type perfect fluid thin disk surrounded by an halo also made of perfect fluid matter embedded in an asymptotic ΛCDM universe. The main physical quantities associated with the disk are

$$\tilde{\sigma} = \frac{\tilde{a}S(t)}{2\pi\left[S(t)\sqrt{\tilde{R}^2 + \tilde{\alpha}^2} + 1\right]^3}, \tag{50a}$$

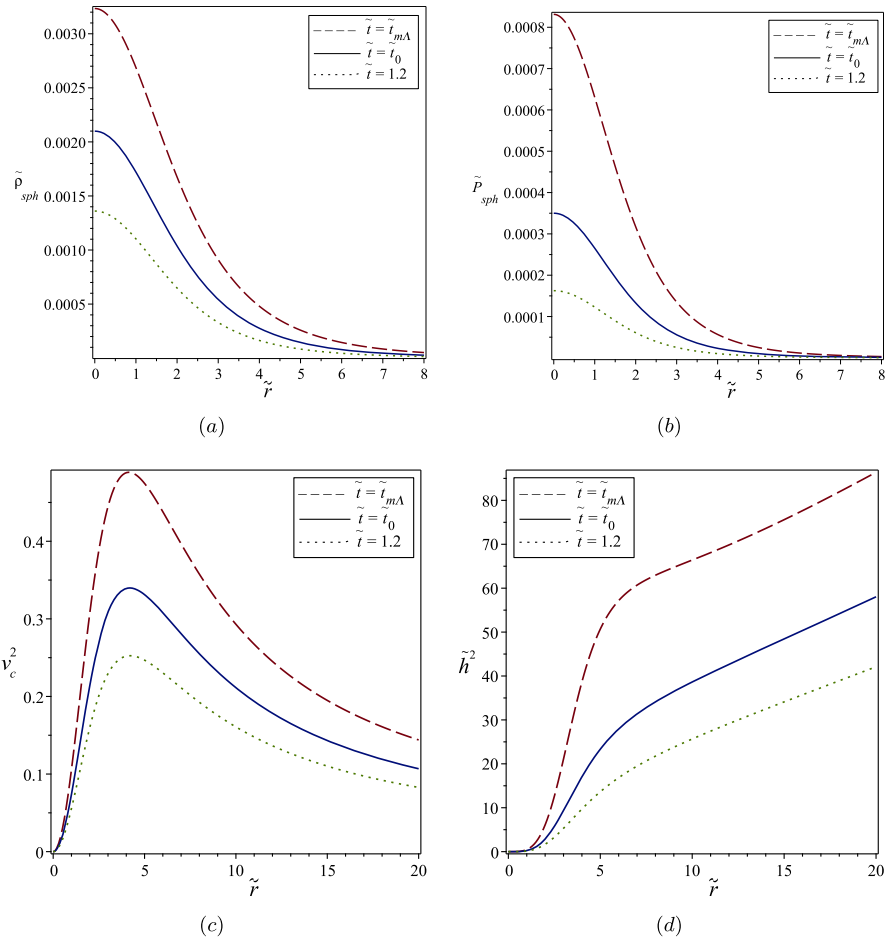

Fig. 2 **a** The energy density $\tilde{\rho}_{\rm sph}$, **b** the pressure $\tilde{P}_{\rm sph}$, **c** the orbital speed v_c^2 and **d** the specific angular momentum $\tilde{h}^2$ for the relativistic Plummer sphere embedded in an asymptotically ΛCDM universe with parameter $\tilde{b}=3$, and the dimensionless cosmic time $\tilde{t}=\tilde{t}_{m\Lambda}$ (dashed curves), $\tilde{t}_0$ (static case, solid curves), and 1.2 (dotted curves), as functions of $\tilde{r}$

$$\tilde{p}=\frac{\tilde{a}S(t)}{4\pi\left[S(t)\sqrt{\tilde{R}^2+\tilde{\alpha}^2}+1\right]^3\left(S(t)\sqrt{\tilde{R}^2+\tilde{\alpha}^2}-1\right)}, \tag{50b}$$

$$v_c^2=\frac{2\tilde{R}^2S(t)\sqrt{\tilde{R}^2+\tilde{\alpha}^2}}{\left[S(t)(\tilde{R}^2+\tilde{\alpha}^2)^{3/2}-\tilde{R}^2+\tilde{\alpha}^2\right]\left(S(t)\sqrt{\tilde{R}^2+\tilde{\alpha}^2}-1\right)}, \tag{50c}$$

$$\tilde{h}^2=\frac{2\tilde{R}^4\left(S(t)\sqrt{\tilde{R}^2+\tilde{\alpha}^2}+1\right)^4}{S(t)^3(\tilde{R}^2+\tilde{\alpha}^2)^{3/2}\left[S(t)^2(\tilde{R}^2+\tilde{\alpha}^2)^2-4S(t)\tilde{R}^2\sqrt{\tilde{R}^2+\tilde{\alpha}^2}+\tilde{R}^2-\tilde{\alpha}^2\right]}, \tag{50d}$$

where the dimensionless quantities and parameters are $\tilde{\sigma} = (r_S^2/M)\sigma$, $\tilde{p} = (r_S^2/M)p$, $\tilde{h} = h/r_S$, $\tilde{R} = R/r_S$, $\tilde{a} = a/r_S$ and $\tilde{\alpha} = \sqrt{\tilde{a}^2 + \tilde{b}^2}$. Equations (50a) and (50b) imply that the weak energy condition is always satisfied, while the strong and dominant energy conditions are satisfied in all the disk if holds the inequality $\tilde{\alpha} \geq 3/(2\,S(t))$, with $S(t) \neq 0$. This condition also implies that we have pressure everywhere of the disk and the stresses associated with the halo and interaction term with the cosmological medium are also positive and non-singular quantities. For disks that asymptotes to the de Sitter spacetime we have $\tilde{\alpha} \geq (3/2)e^{\tilde{t}_0}$. So given a value of the parameters $\tilde{a}$ and $\tilde{b}$, physically realistic disk-like matter distributions with haloes are only possible from some minimum time $S(t^*) = 3/(2\tilde{\alpha})$. However, such structures are still possible for times $t < t^*$ by increasing the parameters $\tilde{a}$ and $\tilde{b}$. It also means that physically acceptable Plummer-type perfect fluid disks with haloes in an expanding universe with a larger length scale today could be older.

In order to study the physical behavior of above quantities we perform a graphical analysis of them for the Plummer-type perfect fluid thin disk surrounded by an halo also made of a perfect fluid embedded in an asymptotically ΛCDM universe with parameters $\tilde{a} = 3$ and $\tilde{b} = 1$ at the dimensionless cosmic times $\tilde{t} = \tilde{t}_{m\Lambda}, \tilde{t}_0$ (static case), and 1.2. In Fig. 3 we plot, as functions of $\tilde{R}$, the surface energy density $\tilde{\sigma}$, the isotropic pressure $\tilde{p}$, the relativistic rotation curves v_c^2 and the specific angular momentum $\tilde{h}^2$. We see that these functions present a similar behavior to previous model. Indeed, we also observer here that these quantities decrease everywhere on the disk during expansion and exhibits at all times a behavior similar to the static case. However, the inclusion of the halo to the disk further decreases the expressions during expansion and also allows us to build disk models with a physically reasonable behavior for earlier times. So for these parameter values $\tilde{t}^* = 0.3771357785$, but as mentioned above physically realistic disks can still be obtained for $t < t^*$ increasing the parameters $\tilde{a}$ and $\tilde{b}$. For example, for the disk with $\tilde{a} = 3$ and $\tilde{b} = 1.6$ obtains that $\tilde{t}^* \approx 0.34$ which corresponds approximately to the epoch of formation of the Galactic thin disk [61]. Also here, for the same value of the parameters, the circular speed of the particles on the plane of the disk is always less than light speed (dominant energy condition), and we have stable circular orbits against radial perturbation. Moreover, the inclusion of the halo to the disk allows us have subluminal rotation curves and photonic orbits for earlier times, and circular orbits more stable. The same behavior is observed for other values of parameters.

6 Miyamoto–Nagai-type anisotropic thick disks embedded in a ΛCDM universe

The application of the Miyamoto–Nagai transformation to the zeroth order Kuzmin–Toomre disk yields the first Miyamoto–Nagai potential-density pair [50, 51]

$$\Phi = -\frac{GM}{\sqrt{R^2 + \left(a + \sqrt{z^2 + b^2}\right)^2}}, \tag{51a}$$

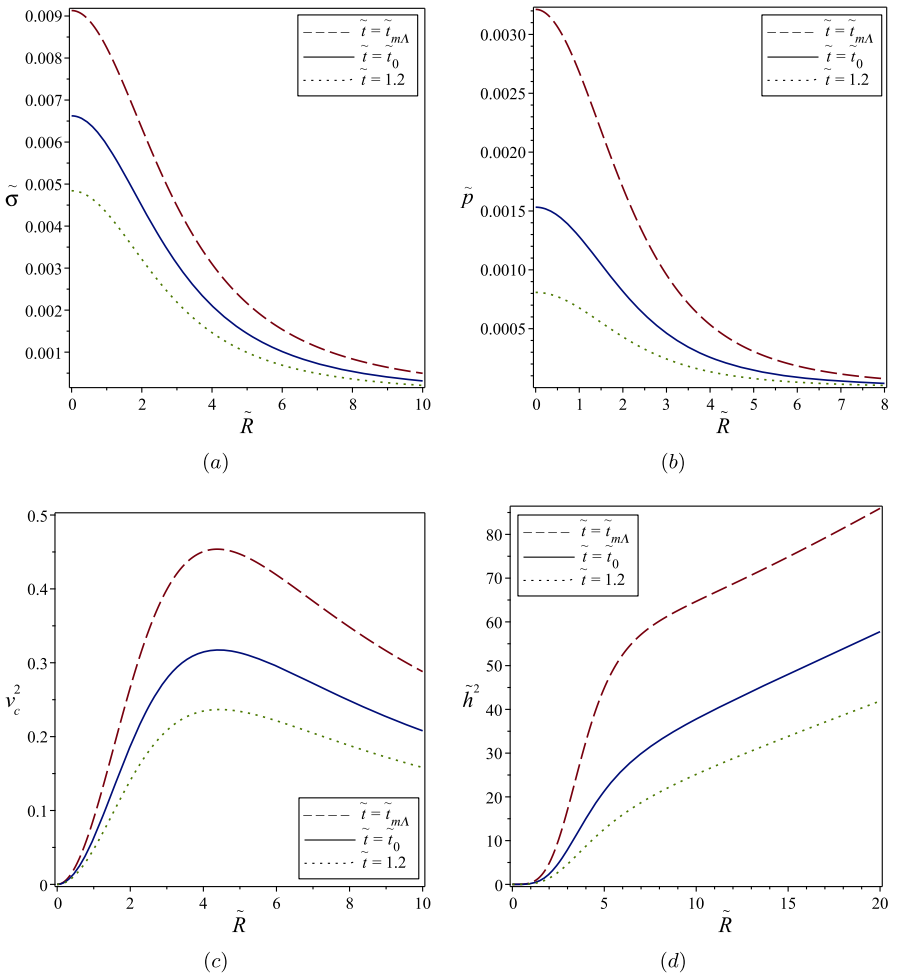

Fig. 3 **a** The surface energy density $\tilde{\sigma}$, **b** the pressure $\tilde{p}$, **c** the relativistic rotation curves v_c^2 and **d** the specific angular momentum $\tilde{h}^2$ for the relativistic Plummer-type thin disk with halo made of a perfect fluid embedded in an asymptotically ΛCDM universe with parameters $\tilde{a} = 3$ and $\tilde{b} = 1$, at the dimensionless cosmic time $\tilde{t} = \tilde{t}_{m\Lambda}$ (dashed curves), $\tilde{t}_0$ (static case, solid curves), and 1.2 (dotted curves), as functions of $\tilde{R}$

$$\rho_N = \frac{b^2 M \left[aR^2 + (a + 3\sqrt{z^2 + b^2})(a + \sqrt{z^2 + b^2})^2 \right]}{4\pi \left[R^2 + \left(a + \sqrt{z^2 + b^2} \right)^2 \right]^{5/2} (z^2 + b^2)^{3/2}}, \tag{51b}$$

where the parameter a, b and M are the length, height scales and the mass of the disk like distribution. The Miyamoto–Nagai potential is used in Newtonian gravity to model the thick disk of spiral galaxies. The Newtonian circular speed on the equatorial

plane is given by

$$v_N^2 = \frac{GMR^2}{\left[R^2+(a+b)^2\right]^{3/2}}. \tag{52}$$

The relativistic expressions for the energy density profile and the principal stresses are

$$\bar{\rho} = \Omega_\Lambda \coth^2\left[\frac{3}{2}\sqrt{\Omega_\Lambda}H_0 t\right] + \frac{2GM\tilde{b}^2 S(t)^2\left[\tilde{a}\tilde{R}^2+(\tilde{a}+3\zeta)(\tilde{a}+\zeta)^2\right]}{3H_0^2 r_S^3\zeta^3\left[f^{-1}+1\right]^5} \tag{53a}$$

$$\bar{P}_\varphi = \bar{P}_R = -\Omega_\Lambda + \left(\frac{2}{f^{-1}-1}\right)\Omega_m S(t)^{-3} + \frac{GM\tilde{b}^2 S(t)^2\left[\tilde{a}\tilde{R}^2+(\tilde{a}+2\zeta)(\tilde{a}+\zeta)^2\right]}{3H_0^2 r_{S(t)}^3\zeta^3\left[f^{-1}+1\right]^5\left[f^{-1}-1\right]}, \tag{53b}$$

$$\bar{P}_z = -\Omega_\Lambda + \left(\frac{2}{f^{-1}-1}\right)\Omega_m S(t)^{-3} + \frac{2GM\tilde{b}^2 S(t)^2(\tilde{a}+\zeta)^2}{3H_0^2 r_S^3\zeta^2\left[f^{-1}+1\right]^5\left[f^{-1}-1\right]}, \tag{53c}$$

where $\bar{\rho}=\rho/\rho_{cr}$, $\bar{P}_\varphi = P_\varphi/\rho_{cr}$, $\bar{P}_z = P_z/\rho_{cr}$, $\tilde{R}=R/r_S$, $\tilde{z}=z/r_S$, $\tilde{a}=a/r_S$, $\tilde{b}=b/r_S$, $\zeta=\sqrt{\tilde{z}^2+\tilde{b}^2}$ and $f^{-1}=S(t)\sqrt{\tilde{R}^2+(\tilde{a}+\zeta)^2}$. The first terms on the right-hand side of equations above represent the components of the ΛCDM universe, the last terms describe a relativistic expanding thick disk in such universe and the second terms in the stresses represent the interaction between the matter of the cosmological medium and the expanding disk. So the energy-momentum tensor can be written as $T_{ab} = T_{ab}^{\Lambda\text{CDM}} + T_{ab}^{\text{int}} + T_{ab}^{\text{disk}}$ and the spacetime can be interpreted as an expanding anisotropic thick disk in a ΛCDM universe. We see that the energy density always is a positive quantity while the inhomogeneous terms in the pressure are positive and non-singular quantities for $\tilde{a}+\tilde{b} > 1/S(t)$. For thick disks that asymptotes to the de Sitter universe we have $\tilde{a}+\tilde{b} > e^{\tilde{t}_0}$. In turn, the circular speed and the specific angular momentum for equatorial orbits are given by

$$v_c^2 = \frac{2\tilde{R}^2 S(t)\sqrt{\tilde{R}^2+\tilde{d}^2}}{\left[S(t)(\tilde{R}^2+\tilde{d}^2)^{3/2}-\tilde{R}^2+\tilde{d}^2\right]\left[S(t)\sqrt{\tilde{R}^2+\tilde{d}^2}-1\right]}, \tag{54a}$$

$$\tilde{h}^2 = \frac{2\tilde{R}^4\left(S(t)\sqrt{\tilde{R}^2+\tilde{d}^2}+1\right)^4}{S(t)^3(\tilde{R}^2+\tilde{d}^2)^{3/2}\left(S(t)^2(\tilde{R}^2+\tilde{d}^2)^2-4\tilde{R}^2 S(t)\sqrt{\tilde{R}^2+\tilde{d}^2}+\tilde{R}^2-\tilde{d}^2\right)}, \tag{54b}$$

where $\tilde{h}=h/r_S$ and $\tilde{d}=\tilde{a}+\tilde{b}$.

In Fig. 4 we plot, as functions of $\tilde{R}$ and $\tilde{z}$, the relativistic density profile $\tilde{\rho}_{\text{d}} = (r_S^3/M)\rho_{\text{d}}$, the pressures $\tilde{P}_{\varphi(\text{d})} = (r_S^3/M)P_{\varphi(\text{d})}$ and $\tilde{P}_{z(\text{d})} = (r_S^3/M)P_{z(\text{d})}$, and in Fig. 5

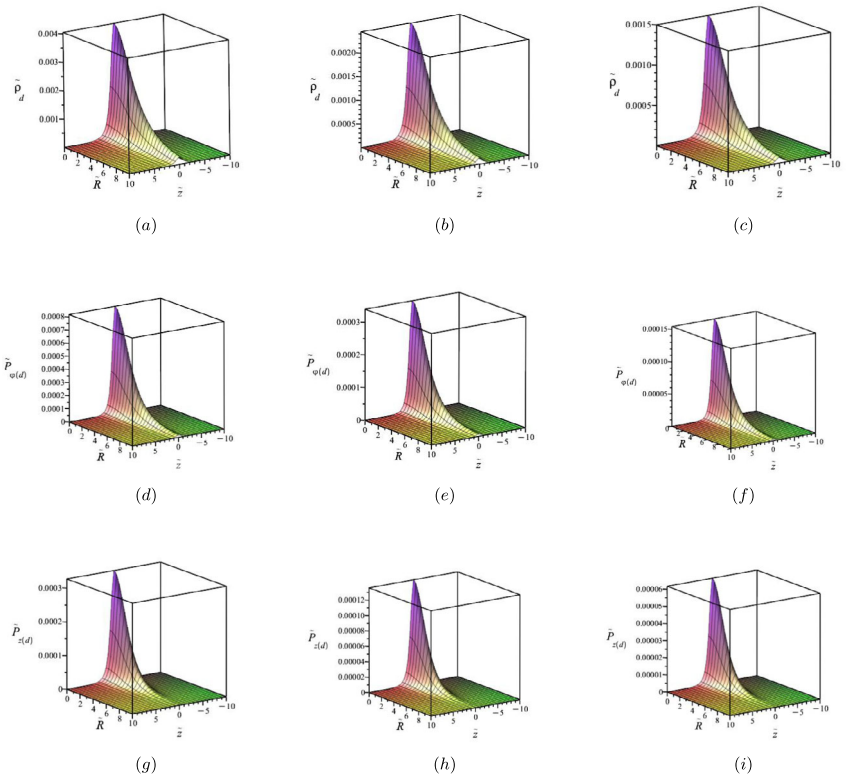

Fig. 4 **a–c** Relativistic density profiles $\tilde{\rho}_{\mathrm{d}}$, the pressures **d–f** $\tilde{P}_{\varphi(\mathrm{d})}$ and (g) - (i) $\tilde{P}_{z(\mathrm{d})}$ for the Miyamoto–Nagai-type thick disk embedded in an asymptotically ΛCDM universe with parameters $\tilde{a} = 3$ and $\tilde{b} = 1$, at the dimensionless cosmic time $\tilde{t} = \tilde{t}_{m\Lambda}$, $\tilde{t}_0$, and 1.2, respectively, as functions of $\tilde{R}$ and $\tilde{z}$

shows, as function $\tilde{R}$, the circular speed profiles v_c^2 and the specific angular momentum $\tilde{h}^2$, for the Miyamoto–Nagai-type thick disk embedded in an asymptotically ΛCDM universe with parameters $\tilde{a} = 3$ and $\tilde{b} = 1$ at the dimensionless cosmic times $\tilde{t} = \tilde{t}_{m\Lambda}$, $\tilde{t}_0$ (static case), and 1.2. We observer that as the universe expands, the above physical quantities decrease everywhere on the disk, but exhibits at all times a behavior similar to the static case, and the inclusion of the thickness to the disk further decreases these quantities and also produces more stable circular orbits. The same behavior is observed for other values of parameters $\tilde{a}$ and $\tilde{b}$.

7 Expanding adiabatic thick spherical shells

In spherical coordinates (t, r, θ, φ) the metric (3) takes the form

$$ds^2 = -\left(\frac{1-f}{1+f}\right)^2 dt^2 + (1+f)^4\, S(t)^2((dr^2 + r^2 d\Omega^2)), \tag{55}$$

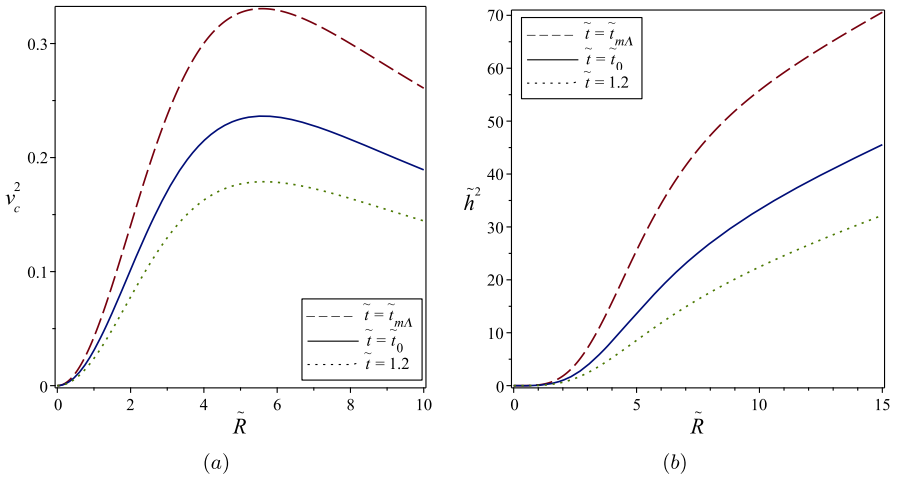

Fig. 5 **a** Relativistic circular speed profiles v_c^2 and **b** the specific angular momentum $\tilde{h}^2$ for the Miyamoto–Nagai-type thick disk embedded in an asymptotically ΛCDM universe with parameters $\tilde{a} = 3$ and $\tilde{b} = 1$, at the dimensionless cosmic time $\tilde{t} = \tilde{t}_{m\Lambda}$ (dashed curves), $\tilde{t}_0$ (static case, solid curves), and 1.2 (dotted curves), as functions of $\tilde{R}$

where $f(r, t)$. The Einstein's gravitational field equations yield the following non-zero components of the energy-momentum tensor

$$8\pi G T^t_t = -3H^2 + \frac{4(f'' + 2r^{-1}f')}{S(t)^2(1+f)^5}, \tag{56a}$$

$$8\pi G T^r_r = -3H^2 - 2\dot{H}\left(\frac{1+f}{1-f}\right) - \frac{4(f'^2 + r^{-1}ff')}{S(t)^2(1+f)^5(1-f)}, \tag{56b}$$

$$8\pi G T^\theta_\theta = 8\pi G T^\varphi_\varphi = -3H^2 - 2\dot{H}\left(\frac{1+f}{1-f}\right) + \frac{2(f'^2 - ff'' - r^{-1}ff')}{S(t)^2(1+f)^5(1-f)}, \tag{56c}$$

where primes indicate differentiation with respect to r. For spacetimes that asymptote to the standard ΛCDM cosmology we have

$$\bar{T}^t_t = -\Omega_\Lambda \coth^2\left[\frac{3}{2}\sqrt{\Omega_\Lambda}H_0 t\right] + \frac{4(f'' + 2r^{-1}f')}{3H_0^2 S(t)^2(1+f)^5}, \tag{57a}$$

$$\bar{T}^r_r = -\Omega_\Lambda + \left(\frac{2}{f^{-1}-1}\right)\Omega_m S(t)^{-3} - \frac{4(f'^2 + r^{-1}ff')}{3H_0^2 S(t)^2(1+f)^5(1-f)}, \tag{57b}$$

$$\bar{T}^\theta_\theta = \tilde{T}^\varphi_\varphi = -\Omega_\Lambda + \left(\frac{2}{f^{-1}-1}\right)\Omega_m S(t)^{-3} + \frac{2(f'^2 - ff'' - r^{-1}ff')}{3H_0^2 S(t)^2(1+f)^5(1-f)}, \tag{57c}$$

where $\bar{T}^a_b = T^a_b/\rho_{cr}$. For the particular form $f = -\frac{\phi(r)}{2S(t)}$ the energy density is again given by the Poisson type non-static and non-linear equation (11), then the metric potential ϕ can be chosen as $\phi = \Phi$ and the pair (Φ, ρ_N) is solution of the equation. Similarly, the circular speed, the specific angular momentum and the stability condition of the particles against radial perturbations are given by (26), (29) and (27), respectively.

As a simple example, we consider the Newtonian potential-density pair [64, 65]

$$\Phi_N = -\frac{GM}{(r^n + b^n)^{1/n}}, \tag{58a}$$

$$\rho_N = \frac{M(n+1)b^n r^{n-2}}{4\pi(r^n + b^n)^{2+1/n}}, \tag{58b}$$

where n is a positive real parameter and b is a non-zero constant with the dimension of length. The models with $0 < p \leq 2$ have a cusp-like density profile and are used as representations of galactic nuclei. In particular, the case $n = 1$ corresponds to the Hernquist model [66] and is used to represent the stellar distribution in spheroidal elliptical galaxies and bulges. The case $n = 2$ is the Plummer model which has a finite central density. So the above potential-density pair is a generalization of Plummer model. The models with $n > 2$ have a density profile that vanishes at the origin and increases outwards near the center, which suggests a shell-like matter distribution. When $n \to \infty$ we have a thin shell of mass M and radius a.

The relativistic expressions for the main physical quantities associated with the matter distributions are

$$\bar{\rho} = \Omega_\Lambda \coth^2\left[\frac{3}{2}\sqrt{\Omega_\Lambda} H_0 t\right] + \frac{2(n+1)MG\tilde{b}^n S(t)^2 \tilde{r}^{n-2} d^{2(2-n)}}{3H_0^2 r_S^3 (S(t)d+1)^5}, \tag{59a}$$

$$\bar{p}_r = -\Omega_\Lambda + \left(\frac{2}{S(t)d-1}\right)\Omega_m S(t)^{-3} + \frac{2MG\tilde{b}^n S(t)^2 \tilde{r}^{n-2} d^{2(2-n)}}{3H_0^2 r_S^3 (S(t)d+1)^5 (S(t)d-1)}, \tag{59b}$$

$$\bar{p}_\theta = \bar{p}_\varphi = -\Omega_\Lambda + \left(\frac{2}{S(t)d-1}\right)\Omega_m S(t)^{-3} + \frac{nMG\tilde{b}^n S(t)^2 \tilde{r}^{n-2} d^{2(2-n)}}{3H_0^2 r_S^3 (S(t)d+1)^5 (S(t)d-1)}, \tag{59c}$$

where $\tilde{r} = r/r_S$, $\tilde{b} = b/r_S$, and $d = (\tilde{r}^n + \tilde{b}^n)^{1/n}$. The first terms on the right-hand side of equations above represent the components of the ΛCDM universe, the last terms describe for $n > 2$ a relativistic expanding adiabatic thick spherical shell in such universe and the second term in pressure represents the interaction between the matter of the cosmological medium and the shell. So the energy-momentum tensor can be written as $T_{ab} = T^{\Lambda\text{CDM}}_{ab} + T^{\text{int}}_{ab} + T^{\text{shell}}_{ab}$ and the solution can be interpreted as an expanding thick spherical shell in a ΛCDM universe. We observer that the energy density always is a positive quantity in accordance with the weak energy condition while the strong and dominant energy conditions are satisfied in all the expanding

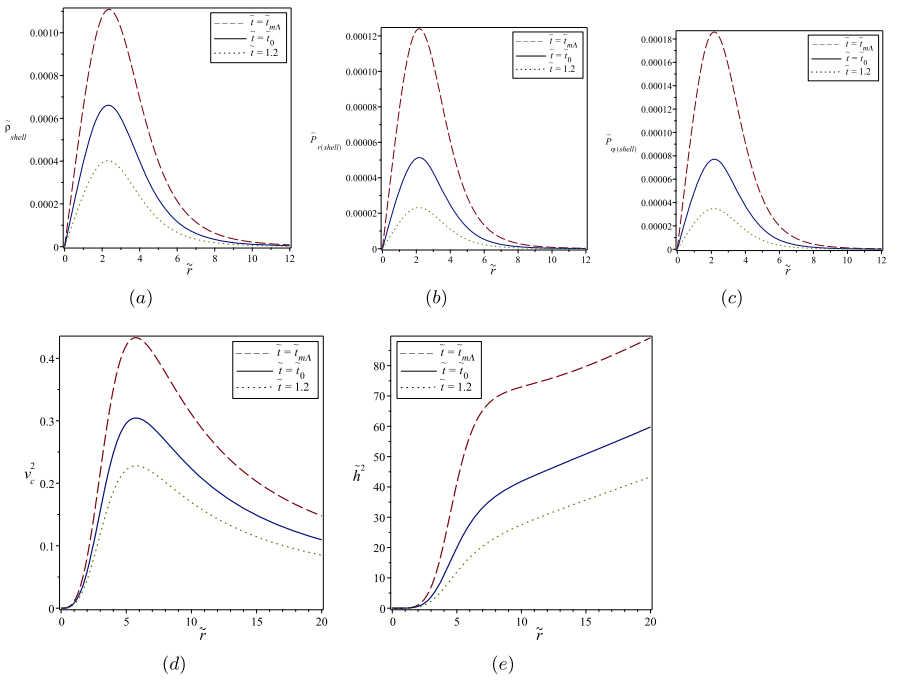

Fig. 6 The relativistic density profile $\tilde{\rho}_{\text{shell}}$, the radial pressure $\tilde{P}_{r(\text{shell})}$, the tangential pressure $\tilde{P}_{\varphi(\text{shell})}$, the circular speed profile v_c^2 and the specific angular momentum $\tilde{h}^2$, for the thick spherical shell embedded in an asymptotically ΛCDM universe with parameters $\tilde{b}=4$ and $n=3$ at the dimensionless cosmic times $\tilde{t}=\tilde{t}_{m\Lambda}$ (dashed curves), $\tilde{t}_0$ (static case, solid curves), and 1.2 (dotted curves), as functions of $\tilde{r}$

shell if holds the inequality $\tilde{b} \geq (3n+2)/\left(2(n+1)S(t)\right)$, with $S(t) \neq 0$. This condition also implies that the inhomogeneous terms in the stress are positive and non-singular quantities. For shells that asymptotes to the de Sitter universe we have $\tilde{b} \geq (3n+2)e^{\tilde{t}_0}/\left(2(n+1)\right)$. For a value of the parameters $\tilde{b}$, physically realistic shell-like matter distributions are only possible from some minimum time $S(t^*) = (3n+2)/\left(2(n+1)\tilde{b}\right)$. However, such structures are still possible for times $t < t^*$ by increasing the parameters $\tilde{b}$. Conversely, increasing n increases the minimum time t^*. In turn, the tangential speed and the specific angular momentum for circular orbits are given by

$$v_c^2 = \frac{2S(t)\tilde{r}^n d}{\left(S(t)d^{n+1} - \tilde{r}^n + \tilde{b}^n\right)\left(S(t)d - 1\right)}, \tag{60a}$$

$$\tilde{h}^2 = \frac{2\tilde{r}^{n+2}\left(S(t)d+1\right)^4}{S(t)^3 d^3\left(S(t)^2 d^{n+2} - 4S(t)\tilde{r}^n d + \tilde{r}^n - \tilde{b}^n\right)}, \tag{60b}$$

where $\tilde{h} = h/r_S$.

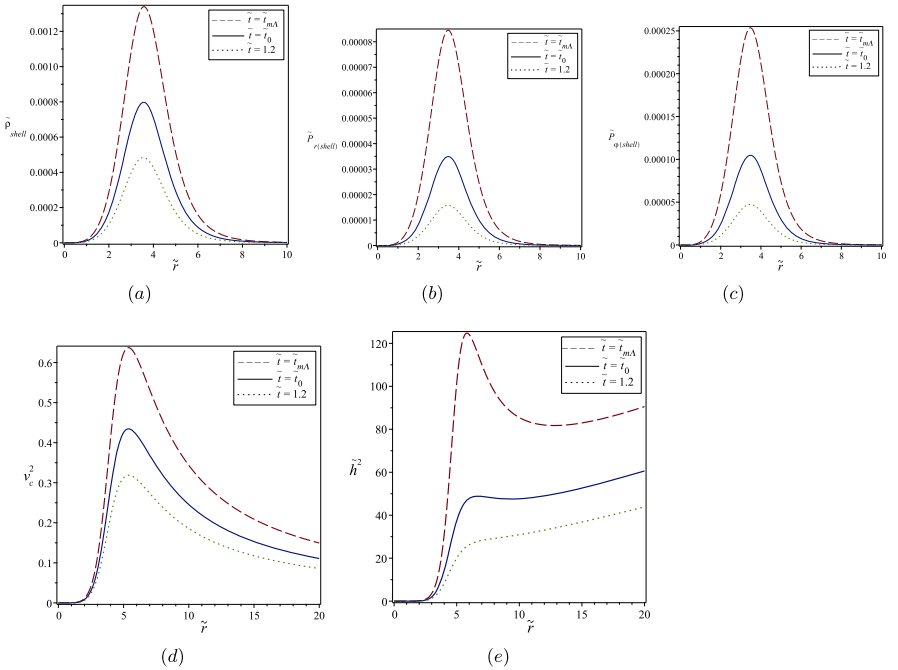

Fig. 7 The relativistic density profile $\tilde{\rho}_{\text{shell}}$, the radial pressure $\tilde{P}_{r(\text{shell})}$, the tangential pressure $\tilde{P}_{\varphi(\text{shell})}$, the circular speed profile v_c^2 and the specific angular momentum $\tilde{h}^2$, for the thick spherical shell embedded in an asymptotically ΛCDM universe with parameters $\tilde{b} = 4$ and $n = 6$ at the dimensionless cosmic times $\tilde{t} = \tilde{t}_{m\Lambda}$ (dashed curves), $\tilde{t}_0$ (static case, solid curves), and 1.2 (dotted curves), as functions of $\tilde{r}$

In Figs. 6 and 7 we present, as functions of $\tilde{r}$, the relativistic density profile $\tilde{\rho}_{\text{shell}} = (r_S^3/M)\rho_{\text{shell}}$, the pressures $\tilde{P}_{r(\text{shell})} = (r_S^3/M)P_{r(\text{shell})}$ and $\tilde{P}_{\theta(\text{shell})} = \tilde{P}_{\varphi(\text{shell})} = (r_S^3/M)P_{\varphi(\text{shell})}$, the circular speed profile v_c^2 and the specific angular momentum $\tilde{h}^2$, for the thick spherical shells embedded in an asymptotically ΛCDM universe with parameters $\tilde{b} = 4$, $n = 3$, and 6, at the dimensionless cosmic times $\tilde{t} = \tilde{t}_{m\Lambda}$, $\tilde{t}_0$ (static case), and 1.2. Just like previous models, we find that as the universe expands, the above physical quantities decrease everywhere on the shells, but exhibits at all times a behavior similar to the static case. We observer that for these parameter values all the energy conditions are satisfied with $\tilde{t}^* = 0.1384213109$ in the case $n = 3$ and $\tilde{t}^* = 0.2514260276$ in the case $n = 6$ and subluminal circular orbits are obtained. We also see that as the parameter n is increased, the shells become more concentrated and the orbits more relativistic but stable orbits against radial perturbations are obtained at later times. Indeed, the shell with $n = 6$ at $\tilde{t}_{m\Lambda}$ presents a region of instability near the center. The same behavior is observed for other values of parameters.

8 Conclusions

Non-static adiabatic axisymmetric structures embedded in an asymptotically ΛCDM universe were constructed from several Newtonian potential-density pairs, using a particular form of the metric in isotropic coordinates. The method was used in building of a perfect fluid thin disk source for the McVittie solution, a system composite by a Plummer-type perfect fluid thin disk surrounded by an halo also made of perfect fluid matter, a model of Miyamoto–Nagai-type anisotropic fluid thick disks, and in the especial case of spherical symmetry, was also presented a family of models of anisotropic thick spherical shells, embedded in an asymptotic ΛCDM universe.

In all case was found that main physical quantities associated with the matter configurations decrease everywhere on the structures during expansion, but exhibit at all times a behavior similar to the static case. Was also observed that expanding physically realistic matter configurations in a ΛCDM universe are only possible from some minimum time. However, such structures are always possible for times less than such time appropriately increasing the parameters. The same behavior was observed for the circular motion of the test particles around of the structures on the equatorial plane and their stability against radial perturbations.

Funding Open Access funding provided by Colombia Consortium

References

1. Peebles, P.J.E.: MNRAS **526**, 4490 (2023)
2. Tully, R.B.: ApJ **257**, 389 (1982)
3. Tully, R.B., et al.: ApJ **676**, 184 (2008)
4. Einasto, M., et al.: A&A **587**, A116 (2016)
5. Tully, R.B., Howlett, C., Pomarède, D.: ApJ **954**, 1 (2023)
6. Cooperstock, F.I., Faraoni, V., Vollick, D.N.: Astrophys. J. **503**, 61 (1998)
7. Bonnor, W.B.: Class. Quantum Grav. **16**, 1313 (1999)
8. Bonnor, W.B.: Class. Quantum Grav. **17**, 2739 (2000)
9. Carrera, M., Giulini, D.: Rev. Modern Phys. **82**, 169 (2010)
10. Giulini, D.: Stud. Hist. Philos. Sci. B **46**, 24 (2014)
11. Agatsuma, K.: Phys. Dark Universe **30**, 100732 (2020)
12. Spengler, F., Belenchia, A., Rätzel, D., Braun, D.: Class. Quantum Grav. **39**, 055005 (2022)
13. Toxvaerd, S.: Class. Quantum Grav. **39**, 225006 (2022)
14. Bonnor, W.A., Sackfield, A.: Commun. Math. Phys. **8**, 338 (1968)
15. Morgan, T., Morgan, L.: Phys. Rev. **183**, 1097 (1969)
16. Morgan, L., Morgan, T.: Phys. Rev. D **2**, 2756 (1970)
17. Lynden-Bell, D., Pineault, S.: Mon. Not. R. Astron. Soc. **185**, 679 (1978)
18. Chamorro, A., Gregory, R., Stewart, J.M.: Proc. R. Soc. Lond. **A413**, 251 (1987)
19. Letelier, P.S., Oliveira, S.R.: J. Math. Phys. **28**, 165 (1987)

20. Lemos, J.P.S.: Class. Quantum Grav. **6**, 1219 (1989)
21. Bičák, J., Lynden-Bell, D., Katz, J.: Phys. Rev. D **47**, 4334 (1993)
22. Bičák, J., Lynden-Bell, D., Pichon, C.: Mon. Not. R. Astron. Soc. **265**, 126 (1993)
23. González, G.A., Espitia, O.A.: Phys. Rev. D **68**, 104028 (2003)
24. Bičák, J., Ledvinka, T.: Phys. Rev. Lett. **71**, 1669 (1993)
25. González, G.A., Letelier, P.S.: Phys. Rev. D **62**, 064025 (2000)
26. Lemos, J.P.S., Letelier, P.S.: Class. Quantum Grav. **10**, L75 (1993)
27. Lemos, J.P.S., Letelier, P.S.: Phys. Rev. D **49**, 5135 (1994)
28. Vogt, D., Letelier, P.S.: Phys. Rev. D **68**, 084010 (2003)
29. Feinstein, A., Ibáñez, J., Lazkoz, R.: ApJ **495**, 131 (1998)
30. González, G.A., Letelier, P.S.: Phys. Rev. D **69**, 044013 (2004)
31. Vogt, D., Letelier, P.S.: MNRAS **363**, 268 (2005)
32. García-Reyes, G., Hernández-Gómez, K.A.: Int. J. Mod. Phys. D **27**(7), 1850068–1 (2018)
33. Vogt, D., Letelier, P.S.: Phys. Rev. D **76**, 084010 (2007)
34. Vogt, D., Letelier, P.S.: MNRAS **402**(2), 1313 (2010)
35. García-Reyes, G.: Gen. Relativ. Gravit. **49**(3), 1 (2017)
36. García-Reyes, G.: Chin. J. Phys. **77**, 465 (2022)
37. Kramer, D., Stephani, H., Herlt, E., McCallum, M.: Exact Solutions of Einsteins's Field Equations. Cambridge University Press, Cambridge (1980)
38. Kustaanheimo, P., Qvist, B.: Gen. Relativ. Gravit. **30**(4), 663 (1998)
39. Nariai, H.: Prog. Theor. Phys. **38**(1), 92 (1967)
40. Planck Collaboration: N. Aghanim, Y. Akrami, et al., A&A **641**, A6 (2020)
41. Frieman, J.A., Turner, M.S., Huterer, D.: Annu. Rev. Astron. Astrophys. **46**, 385 (2008)
42. Ryden, B.: Introduction of Cosmology. Cambridge University Press, Cambridge (2017)
43. Hawking, S.W., Ellis, G.F.R.: *The Large Scale Structure of Spacetime* (Cambridge University Press, Cambridge, UK, p. 88) (1973)
44. Binney, J., Tremaine, S.: Galactic Dynamics, 2nd edn. Princeton Univ. Press, Princeton (2008)
45. Rayleigh, Lord: Proc. R. Soc. Lond. A **93**, 148 (1917)
46. Landau, L.D., Lifshitz, E.M.: Fluid Mechanics (Addison-Wesley, Reading, MA) (1989)
47. Letelier, P.S.: Phys. Rev. D **68**, 104002 (2003)
48. Kuzmin, G.: Astron. Zh. **33**, 27 (1956)
49. Toomre, A.: Astrophys. J. **138**, 385 (1962)
50. Miyamoto, M., Nagai, R.: PASJ **27**, 533 (1975)
51. Nagai, R., Miyamoto, M.: PASJ **28**, 1 (1976)
52. Papapetrou, A., Hamouni, A.: Ann. Inst. Henri Poincaré **9**, 179 (1968)
53. Lichnerowicz, A.: C.R. Acad. Sci. **273**, 528 (1971)
54. Taub, A.H.: J. Math. Phys. **21**, 1423 (1980)
55. Israel, E.: Nuovo Cimento **44B**, 1 (1966)
56. Israel, E.: Nuovo Cimento **48B**, 463 (1967)
57. McVittie, G.C.: Mon. Not. R. Astron. Soc. **93**, 325 (1933)
58. Kaloper, N., Kleban, M., Martin, D.: Phys. Rev. D **81**, 104044 (2010)
59. Lake, K., Abdelqader, M.: Phys. Rev. D **84**, 044045 (2011)
60. Rothman, T., Campbell, M., Goswami, R., Ellis, G.F.R.: Phys. Rev. D **99**, 024033 (2019)
61. del Peloso, E.F., da Silva, L., Porto de Mello, G.F., Arany-Prado, L.I.: A&A **440**, 1153 (2005)
62. Plummer, H.C.: MNRAS **71**, 460 (1911)
63. Buchdahl, H.A.: ApJ **140**, 1512 (1964)
64. Evans, N.W., An, J.: Mon. Not. R. Astron. Soc. **360**, 1 (2005)
65. Vogt, D., Letelier, P.S.: Mon. Not. R. Astron. Soc. **402**, 1313 (2010)
66. Hernquist, L.: Ap. J. **356**, 359 (1990)